

Platinum alloy development—the Pt-Al-Cr-Ni system

J. PREUSSNER*, M. WENDEROTH, S. PRINS†, R. VÖLKL, and U. GLATZEL

*Metals and Alloys, University of Bayreuth, Bayreuth, Germany

†Phases Research Lab, Pennsylvania State University

Platinum base alloys are very corrosion resistant and have got a high melting point. Similar to Ni-base superalloys, which are used for jet turbines, the hardening effect of the intermetallic L_{12} Pt_3Al phase is used to receive a material that is creep resistant at high temperatures. Chromium is added to the alloy system to stabilize the L_{12} phase down to room temperature. With the right amount of nickel the misfit and shape of the precipitates can be controlled.

Various alloy compositions have been melted and analysed. With scanning electron microscopy (SEM) and energy dispersive spectroscopy (EDS) a microstructure can be observed, which is very similar to the one in Ni-base superalloys.

To support alloy development with simulations, a thermodynamic database of the Pt-Al-Cr-Ni system is about to be established. The SEM and EDS measurements provide useful input to the thermodynamic optimization. Also many data from the literature have been used to receive the best approximation. The Cr-Pt binary phase diagram has been reassessed and the latest results of thermodynamic modelling are presented.

Introduction

At the Chair of Metals and Alloys at the University of Bayreuth, precipitation hardened Pt-base alloys are developed. These alloys exhibit good corrosive and creep resistance, which is required for devices that undergo high temperatures such as in the glass industry and for aero- and astronomical engines.

Nickel-base superalloys show excellent creep resistance at high temperatures. They are used for turbine blades where they have to bear high creep loads and the corrosive gas stream. It is possible to copy the very effective strengthening technique of Ni-base superalloys to Pt-base alloys. With platinum-based alloys with a certain amount of aluminium a microstructure of periodically aligned Pt_3Al precipitates with L_{12} crystal structure embedded in a Platinum rich matrix can be achieved, which is shown in Figure 1. With the substitution of the base element Ni with Pt, which has got a higher melting point and is more inert, an even better temperature resistance can be reached. Chromium is added to stabilize the L_{12} phase down to room temperature. With the right amount of nickel the misfit and shape of the precipitates can be controlled.

The development of Pt-base alloys is supported by thermodynamic simulations. Thus, the chemical phases that form at a certain temperature and a certain amount of alloying additions can be predicted. Furthermore, with non-equilibrium calculations that take diffusion into account, it is possible to optimize the heat treatment.

Using the CALPHAD method for Pt-base alloy development

Mechanical, chemical and physical properties of metals are substantially influenced by their microstructure. Therefore knowledge and understanding of the microstructure and its formation is of great interest. With thermodynamic

simulations it is possible to understand and predict the formation of phases.

It is reasonable to describe an alloy system through functions of the Gibbs energy against the concentration of the alloying elements and the temperature $G(x,T)$. If the function of the Gibbs energy is known, all the extensive thermodynamic data of an alloy system can be extrapolated. The stable phases at any temperature and composition of the elements in equilibrium and thus the phase diagram can

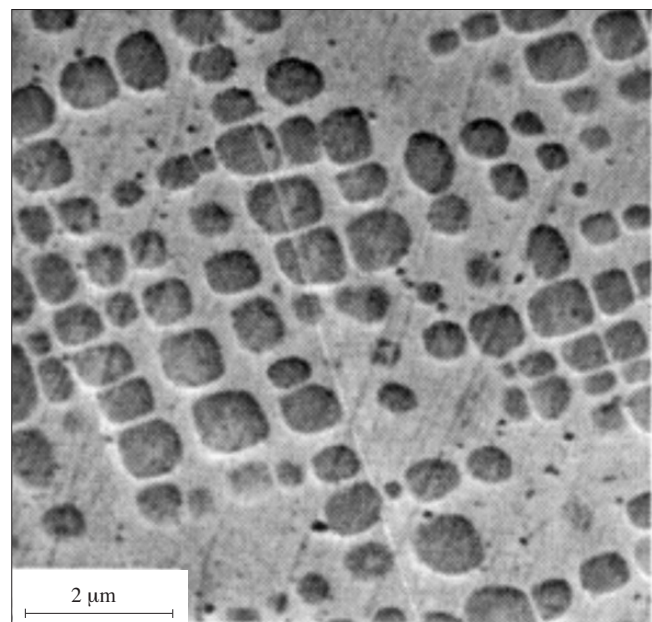


Figure 1. SEM micrograph of a platinum-based alloy $Pt_{77}Al_{14}Cr_3Ni_6$ (heat treated 12 h 1500°C + 120 h 1000°C). A two-phase microstructure of cubic precipitates can be observed

be calculated². The prediction of ternary phase diagrams from binary data is one of the most valuable possibilities of that approach.

To get a good description of the Gibbs energy experimental data (e.g. activity measurements, heat of formation, phase transition temperatures, etc.) can be used for an optimization process.

Thermodynamic description of the binary Cr-Pt system

The Cr-Pt-System has been assessed by Oikawa *et al.*³ previously. This description took into account only the solution phases liquid, Pt solid solution and Cr solid solution and the A15 ordered phase. Furthermore the eutectic temperatures are not in good agreement with¹. Therefore the system has been assessed anew.

The experimental phase diagram is shown in Figure 2. In the Cr-Pt system the phases Cr solid solution with a bcc lattice, Pt solid solution with fcc lattice, the liquid phase, and the ordered phases Cr₃Pt (A15), CrPt (L1₀) and CrPt₃ (L1₂) have been approved.

To get a complete thermodynamic description of the phase diagram the Gibbs energy of every phase needs to be modelled. The solid solution phases can be described by a subregular solution model as described in²:

$$G_m = {}^0 G_{Cr} x_{Cr} + {}^0 G_{Pt} x_{Pt} + RT(x_{Cr} \ln x_{Cr} + x_{Pt} \ln x_{Pt}) + {}^E G_m + {}^{mag} G_m,$$

whereas

$${}^E G_m = {}^0 L_{CrPt} x_{Cr} x_{Pt} + {}^1 L_{CrPt} (x_{Cr} \pm x_{Pt}) x_{Cr} x_{Pt}$$

With the mole fraction x_i and a magnetic contribution of the fcc phase ${}^{mag}G$. The first term describes a mechanical mixing of both components, the second term is an entropy term, which describes the ideal entropy of mixing in a solution. Magnetic contributions can also be considered.

The L parameter of the excess term E_G can be optimized according to experimental data and can be temperature dependent $L=A+BT$. Optimization means that all thermodynamic data which are available for that alloy system, e.g. activity data, enthalpy of mixing and of course temperatures where phase changes occur, can be used to assess the values of L .

The ordered A15 phase has been modelled with the compound energy formalism as shown in².

$$G_m = G_{Cr:Cr} y_{Cr}^I y_{Cr}^{II} + G_{Cr:Pt} y_{Cr}^I y_{Pt}^{II} + L_{Cr:Cr,Pt} y_{Cr}^I y_{Cr}^{II} y_{Pt}^{II} + 1/4RT(y_{Cr}^{II} \ln y_{Cr}^{II} + y_{Pt}^{II} \ln y_{Pt}^{II})$$

Similar to the mole fraction x_i , the occupation of a sublattice s in the crystal with an element A is the site fraction y_A^s . So the atomic fraction of a component on a certain sublattice site in the crystal lattice can be specified. If every site fraction of the lattice y_A^s is equal the phase is disordered².

The Cr-Pt phase diagram shows a Pt solid solution, with an ordering reaction at 'approx' 1130°C to the L1₂/L1₀ phase. This behaviour has also been modelled, with the approach described in⁴. The Gibbs energy of the ordered L1₂ structure G_m^{L12} can be explained by the Gibbs energy of the disordered fcc state G_m^{fcc} plus the molar ordering energy ΔG_m^{L12} .

$$G_m^{L12} = G_m^{fcc}(x_i) + \Delta G_m^{L12}(y_i)$$

$$\Delta G_m^{L12} = G_m^{4sl}(y_i) \pm G_m^{4sl}(y_i = x_i)$$

The ordering energy of the L1₂ structure is given by a four sublattice model⁴.

The parameters after optimization to the experimental values are shown in Table I. The thermodynamic descriptions of the pure elements were taken from the SGTE database⁵.

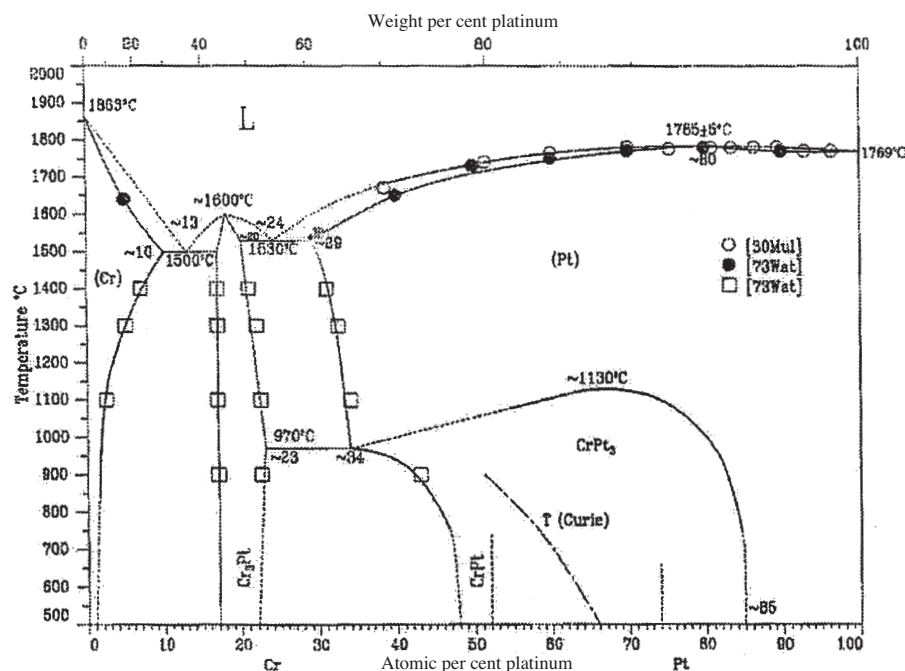


Figure 2. Experimental phase diagram of Cr-Pt¹

First-principle calculations

With the help of first-principle calculations the enthalpy of formation of compounds can be calculated. These calculations are complex and still very time consuming based on density functional theory as described in⁶. As these results are often hard to determine experimentally, this technique is quite powerful. The results can be directly used in a thermodynamic description of the alloy systems⁷. The program VASP⁸ has been used to calculate the enthalpies of formation of the ordered compounds. At this stage no magnetic contribution has been added yet to the calculations. At the L₁₂-ordered CrPt₃ Kussmann *et al.*⁹ observed ferromagnetic behaviour, while Pickard *et al.*¹⁰ observed ferrimagnetic behaviour. The total energies of the pure elements were compared to those obtained by Wang *et al.*¹¹ with very good agreement. The resulting enthalpies of formation are listed in Table I.

Resulting Cr-Pt phase diagram

The phase diagram after a thermodynamic optimization process is shown in Figure 4. The calculated phase diagram shows a very good agreement with experimental data. The modelled eutectic temperatures are within the stated experimental errors. The ordering reaction still needs to be modelled correctly. The missing of the L₁₂ Pt₃Cr phase at low temperatures may be a result of not taking into account the magnetic properties yet. Because all the Gibbs energies have been modelled, it is now possible to derive further thermodynamic data. Figure 4 shows a comparison between the calculated and the experimental chemical activities.

With the use of first principle calculations in the thermodynamic model, it has been found that a Cr₃Pt phase with L₁₂ crystal structure is very likely to form at low temperatures. That gives a hint that the platinum-rich side of the phase diagram should be further examined.

Table I

Assessed thermodynamic parameters of the Cr-Pt system

${}^0L_{PtCr}^{liq} = -372230 + 2.10T$
${}^1L_{PtCr}^{liq} = -51408$
${}^0L_{PtCr}^{bcc} = -341648$
${}^1L_{PtCr}^{bcc} = -5000$
${}^0L_{PtCr}^{fcc} = -369270 + 14T$
${}^1L_{PtCr}^{fcc} = -54591$
$G_{Cr:Cr}^{A15} - 4H_{Cr}^{SER} = 191450 + 4GHSERCR$
$G_{Cr:Pt}^{A15} - 3H_{Cr}^{SER} - H_{Pt}^{SER} = -359750 + 47T$
$+ 3GHSERCR + GHSERPT$
${}^0L_{Cr:Cr,Pt}^{A15} = -544530 + 75T$
$G_{Cr_3Pt}^{A15} = -2516$
$G_{Cr_2Pt_2}^{A15} = -2740$
$G_{CrPt_3}^{A15} = -1404$
${}^0L_{Cr,Pt,Cr,Pt:Cr:Cr}^{ord} = -5000$
${}^0L_{Cr,Pt,Cr,Pt:Cr:Pt}^{ord} = -5000$
${}^0L_{Cr,Pt,Cr,Pt:Pt:Pt}^{ord} = -5000$

The Pt-Al-Cr-Ni system

The thermodynamic assessment of the Cr-Pt system has already shown that many regions of the binary phase diagram are relatively unknown. The *ab initio* calculations for example show that a stable Cr₃Pt-L₁₂ structure is supposable, see Table I and Figure 3. Greenfield and Beck¹⁵ discovered a stable L₁₂ structure at 63 atomic pct. Cr, but the phase is not shown in experimental phase diagrams¹. More experimental work needs to be done to reveal the L₁₂ and L₁₀ phase regions.

The additional alloying elements Cr and Ni have shown that a microstructure similar to those of Ni-base superalloys can be achieved¹⁶. Many experiments on the Pt-rich side of the Pt-Al-Cr-Ni system have already been done. An expansion of the γ' -L₁₂ structure with the addition of nickel

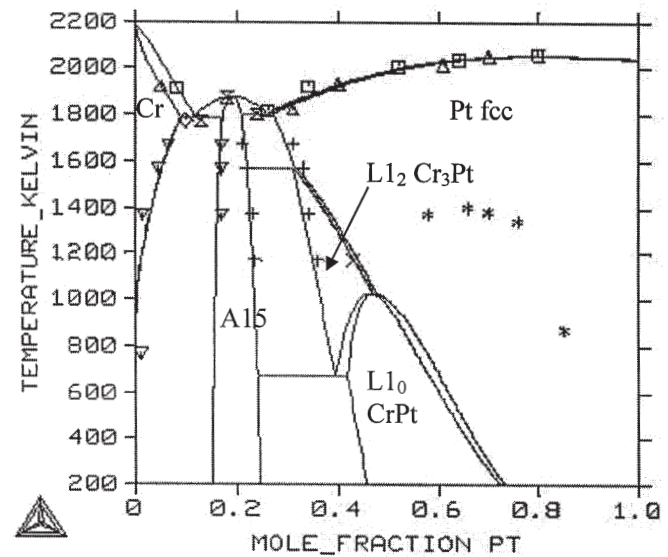


Figure 3. Phase diagram after thermodynamic modelling with the parameters given in Table I. The various symbols are experimental values from ¹ and ¹². The low temperature L₁₂ CrPt₃ phase is not modelled in good agreement yet. *Ab initio* calculations give an indication of a stable L₁₂ Cr₃Pt phase

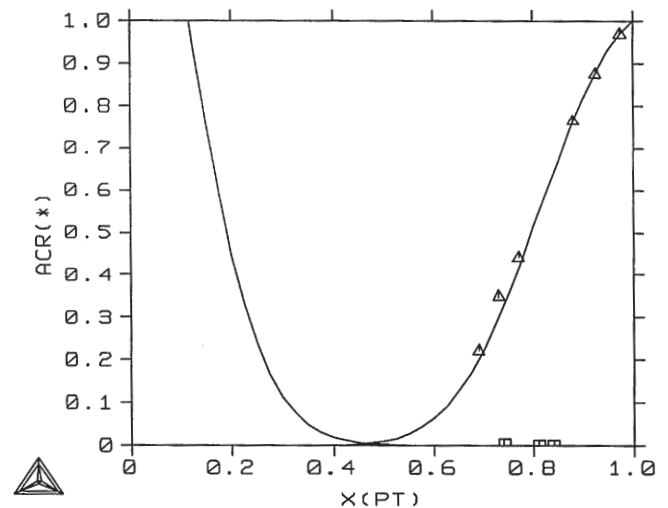


Figure 4. Calculated activity of Cr and Pt at 1500°C (with respect to the pure phases at 1500°C) compared with experimental results from^{13,14}

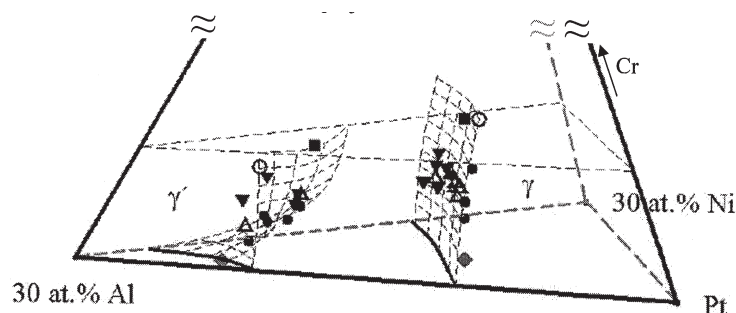


Figure 5. Pt-Al-Cr-Ni phase diagram of the Pt rich side¹⁷

has been observed, see Figure 5¹⁷. The development of a thermodynamic description of the quaternary system for the platinum-rich side with special focus on the L₁ phase region is projected.

Outlook

The use of thermodynamic simulations allows reviewing the experimental measurements, which have been carried out at the alloy system. With the combination of further selective experiments and simulation, a complete thermodynamic description of the system can be achieved. From modelling of further binary data, the ternary phase diagrams can be extrapolated, which gives important information for alloy development. With the merging of multiple binary data the description of the whole Pt-Al-Ni-Cr system with main interest on the platinum-rich side needs to be modelled. The obtained databases can be further used in kinetic simulations.

References

1. VENKATRAMAN, M. and NEUMANN, J.P. *Bull. Alloy Phase Diagrams* 11, 1990. pp. 16–21.
2. HILLERT, M. *Phase Equilibria, Phase Diagrams and Phase Transformation*, Cambridge University Press, Cambridge, UK, 1998.
3. OIKAWA, K., QIN, G.W., IKESHOJI, T., KITAKAMI, O., SHIMADA, Y., ISHIDA, K., FUKAMICHI, K., and *J. Magn. Magn. Mater.* 236, 2001. pp. 220–233.
4. KUSOFFSKY, A., DUPIN, N., and SUNDMAN, B. *CALPHAD* 15, 2001. pp. 549–565.
5. DINSDALE, A.T. *CALPHAD* 15. pp. 317–425
6. KOHN, W., and SHAM, L.J. *Phys. Rev.* 140, 1965, 1991. pp. A1133–1138.
7. WOLVERTON, C., YAN, X.Y., VIJAYARA-
- GHAVAN, R., OZOLINŠ, V. *Acta Mater.* 50, 2002. pp. 2187–2197.
8. KRESSE, G. *VASP, Vienna Ab-initio Package Simulation*, <http://cms.mpi.univie.ac.at/vasp/>, 2004.
9. KUSSMANN, A., MÜLLER, K., and RAUB, E. *Z Metallkd* 59, 1968. pp. 859–863.
10. PICKART, S.F. and NATHANS, R. *J. Appl. Phys.* 33, 1962. pp. 1203–1204.
11. WANG, Y., CURTAROLO, S., JIANG, C., ARROYAVE, R., WANG, T., CEDER, G., CHEN, L.-Q., and LIU, Z.-K. *CALPHAD* 28, 2004. pp. 79–90.
12. WATERSTRAT, R.M. *Metall. Trans.* 4, 1973. pp. 1585–1592.
13. GARBERS-CRAIG, A.M. and DIPPENAAR, R. *J. Met. Mat. Trans. B* 28B, 1997. pp. 547–552.
14. KAY, D.A.R. and MOHANTY, A.K. *Met. Trans.* 1, 1970. pp. 303–304.
15. GREENFIELD, P. BECK, A. *J. Met. Trans. AIME* February, 1956. pp. 265–276.
16. WENDEROTH, M., CORNISH, L.A., SÜSS, R., VORBERG, S., FISCHER, B., GLATZEL, U., and VÖLKL, R. *Metall. Mater. Trans. A*, 36A, 2005. pp. 567–575.
17. VORBERG, S. PhD thesis, Universität Bayreuth, 2006.